Compositional reservoir modeling often requires a large number of instantaneous calculations. To reduce the dimension of the problem and the amount of computation, several components are usually grouped into pseudo-components. However, to model surface processes, it is important to have a detailed phase composition. Accurate fluid composition requires laboratory analysis, which is costly and time-consuming. This study addresses this issue by introducing an advanced delumping procedure aimed at providing an accurate fluid characterization.

The primary objective was to develop a sophisticated delumping procedure capable of precisely describing detailed fluid compositions from calculations involving mixtures. Its goal is to reduce reliance on laboratory analysis, making the process more efficient. The results obtained from this research can improve the planning and modeling of surface facilities, developed under conditions of reservoir pressure above saturation pressure.

To test the effectiveness of the proposed delumping and achieve the goals set, experiments were carried out on compositional simulation of oil production in the Caspian basin. The procedure uses reduction parameters calculated from simulation data and an analytical approach to characterize fluid compositions from the original data. Detailed fluid compositions obtained through laboratory PVT analysis were then compared with the results of simulation using PVTsim software and numerical delumping procedures. The findings showed a close agreement between the outcomes of detailed compositions obtained through the delumping procedure and of laboratory analysis, with an average deviation less than 5 %, confirming the effectiveness of delumping as an alternative method for obtaining an accurate fluid composition

Keywords: delumping, lumping, fluid description, fugacity coefficients, PVTsim software, pseudo-components

UDC 504
DOI: 10.15587/1729-4061.2023.289932

DEVELOPMENT AND APPLICATION OF FLUID CHARACTERIZATION ALGORITHMS TO OBTAIN AN ACCURATE DESCRIPTION OF A PVT MODEL FOR KAZAKHSTANI OIL

Jamilyam Ismailova
PhD, Associate Professor*
Dinara Delikesheva
Master of Technical Sciences, Senior Lecturer*
Aibek Abdukarimov
Master of Engineering, Senior Lecturer**
Nargiz Zhumanbetova
Master of Technical Sciences, Lecturer*
Adel Sarsenova
Corresponding author
Master of Petroleum Engineering, Senior Lecturer**
E-mail: adel.askarbekovna@gmail.com
*Department of Petroleum Engineering
Satbayev University
Satpayev str., 22a, Almaty, Republic of Kazakhstan, 050013
**School of Energy & Petroleum Industry
Kazakh-British Technical University
Tole bi str., 59, Almaty, Republic of Kazakhstan, 050000

Received date 04.08.2023
Accepted date 19.10.2023
Published date 30.10.2023

How to Cite: *Ismailova, J., Delikesheva, D., Abdukarimov, A., Zhumanbetova, N., Sarsenova, A. (2023). Development and application of fluid characterization algorithms to obtain an accurate description of a PVT model for kazakhstani oil. Eastern-European Journal of Enterprise Technologies, 5 (6 (125)), 6–20. doi: https://doi.org/10.15587/1729-4061.2023.289932*

1. Introduction

Delumping techniques are integral to various aspects of petroleum engineering, from reservoir modeling to facility design and environmental management. They enable engineers and researchers to gain a more accurate and detailed understanding of complex hydrocarbon mixtures, facilitating better decision-making and optimization of petroleum industry processes.

Fluid characterization, a fundamental aspect of petroleum engineering, hinges on delumping for obtaining accurate data on hydrocarbon composition, density, viscosity, and other crucial properties. This information guides decisions related to refining, transport, and processing, ensuring that the final products meet industry standards and customer requirements.

Process simulation in the petroleum industry relies on delumping to model complex systems accurately. It facilitates the design and optimization of production processes, ensuring that facilities operate efficiently and cost-effectively. Delumping also contributes to flow assurance, helping to prevent issues such as pipeline blockages and flow instability by providing a comprehensive understanding of the fluid's composition and behavior.

In reservoir modeling, delumping techniques are pivotal for simulating the behavior of complex hydrocarbon reservoirs. By breaking down the reservoir fluid into its individual components, engineers can gain insights into fluid properties, phase behavior, and composition, leading to more accurate predictions of reservoir performance. This, in turn, aids in optimizing production strategies and maximizing resource recovery.

When modeling a compositional reservoir, a significant number of instantaneous calculations are required, leading to high computational costs. As a result, the fluid description used in these models is often simplified and includes only a small number of components or pseudo-components. This simplification process, known as "lumping", involves grouping certain components from a more detailed fluid description [1, 2].

The detailed description of the fluid is typically obtained using analytical methods such as chromatography, which can effectively identify and separate low-molecular-weight components. However, high-molecular-weight components are usually grouped based on specific properties such as boiling temperature range, number of carbon atoms, chemical family, etc. By grouping these components, the computational complexity of reservoir modeling is reduced while preserving the fundamental behavior of the liquid system [3].

Since the results provided by compositional modeling only allow you to obtain the average values of pseudo-components in C7+ fractions, it is necessary to do the reverse procedure of ungrouping or delumping in other words, which ensures the compositional behavior of the detailed liquid as a result of the flash calculation outcomes for the purposes of not only planning but also modeling of surface facilities. Such studies are the most important for the oil of the Caspian region including giant fields where calculations of phase equilibrium, refinement of composition and planning of ground facilities will benefit from reducing uncertainty and increasing the accuracy of the compositional data for the design of facilities. For the Caspian basin, a method is proposed that is based on a modified method – a method for ungrouping a mixed mixture that considers non-zero parameters of the binary interaction parameters. The delumping of composite modeling results will ensure an increase in the accuracy of calculations when modeling surface facilities.

Although various delumping methods have been proposed for determining detailed fluid composition, there is a notable lack of comprehensive studies evaluating their efficiency and robustness as a viable replacement for expensive laboratory analysis. Hence, the research addresses several critical issues, including:

1. Lack of Detailed Fluid Description: The existing compositional reservoir modeling often relies on simplified fluid descriptions with a limited number of components or pseudo-components. This simplification may not capture the detailed phase composition of crude oil accurately.

2. Reliance on Expensive Laboratory Analysis: Achieving accurate fluid composition typically requires labor-intensive and costly laboratory PVT analysis. This reliance on laboratory analysis can be impractical and time-consuming, particularly for oil production planning in regions like the Caspian basin.

3. Need for Detailed Phase Composition: Accurate modeling of surface processes in oil production requires a detailed understanding of the phase composition of the reservoir fluid. This level of detail is often lacking in simplified fluid descriptions.

4. Effectiveness of Delumping Procedure: While delumping procedures have been proposed to evaluate detailed phase compositions from instantaneous calculations on mixed mixtures, their efficiency for laboratory analysis needs to be rigorously evaluated.

5. Enhancing Oil Production Planning: Improving the planning and modeling of onshore facilities for oil production in the Caspian basin, a region known for its giant oilfields, requires reducing uncertainty and enhancing the accuracy of compositional data for facility design.

Therefore, research on the development and validation of advanced delumping procedures in petroleum engineering is undeniably relevant. By improving fluid characterization, reducing computational burdens, and enhancing the accuracy of phase composition data, this research directly contributes to the effectiveness and reliability of simulation studies. Moreover, it offers a practical alternative to the heavy reliance on costly and time-consuming laboratory analysis.

2. Literature review and problem statement

Scientists have been developing and studying different ways to take a simplified description of a fluid and turn it into a more detailed one. They have been working on different methods to get the most accurate. The earliest research on delumping with great precision was presented in the paper [3]. The authors calculated the detailed composition using the material balance after approximating the detailed component K-values using the lumped component liquid vapor equilibrium composition, split parameters, and detailed EOS parameters. They selected calibration points in a ternary interpretation between the oil and gas compositions, however, no details regarding the anticipated composition trend were provided. Moreover, the characterization of the fluid in terms of real components was not explored in this work, which makes relevant research impractical.

Then, in the literature source [4], the authors adopted the approach based on Michelson's simplified flash and modified Wilson's equation. They used a material balance to obtain the precise compositions of the relevant phases after determining the research K-values of the original components as a function of the EOS parameters. For constant temperature and pressure conditions, the logarithmic form of each component's K-value correlates with its acentric factor and reduced temperature. This method demonstrated significant improvement in predicting results for gas injection processes. However, it's important to note that the reduction in CPU time resulting from lumping can also be accompanied by a loss of information. Thus, it is important to do further investigation for increasing the delumping procedure's effectiveness.

In the study [5], a similar strategy was presented, with the exception that K-values were linked to the EOS parameters 'a' and 'b'. According to their method, known as the LSK (Leibovici-Stenby-Knudsen) algorithm, the lumping process begins by flashing the lumped system under relevant conditions to calculate the K-values for the lumped components. The K-values of the original components can be calculated using these constants, and the Rachford-Rice equation can then be used to compute phase fractions and phase mole fractions. Their method was based on the linear relation of the logarithm of the K-value with equation of state parameters when all binary interaction coefficients are equal to zero.

The temperature, pressure, and phase parameters are complicated functions of the equation's C_k coefficients. Where C_i is the equation of state parameters and 'a_i' and 'b_i' are constants. The constants of this equation can be computed analytically when all binary interaction coefficients are

equal to zero. However, the equation is approximate when non-zero interactions are present, and the constants must be found using the regression approach.

A new approach for delumping of a compositional reservoir simulation was described in the paper [6]. The approach was based on a recently released method for delumping the results of a single flash phase equilibrium computation. The scientists assumed that for each detailed component, time step and grid block, the total quantity of fluid moles and total mole percentage were known. The oil and gas molar fluxes between adjacent grid blocks were also known. Notably, this approach has been effectively utilized to design and optimize distillation columns in petrochemical and refining processes. Nevertheless, its accuracy is significantly decreased in the presence of nonzero BICs. This highlights the importance of considering complexities associated with fluid behavior in a reservoir, as nonzero BICs are commonly encountered in real fluid systems.

The algorithm, as described in [7], facilitates the precise calculation of fluid composition generated from individual wells within each time step. This method stands out as an improvement over the previous one due to its ability to effectively handle scenarios involving non-zero binary interaction coefficients (BICs). However, despite these promising developments, there remain unresolved issues related to the practical implementation of this algorithm. These issues might stem from objective difficulties related to the computational complexity of the calculations, the inherent impossibility of achieving perfect accuracy in real-world scenarios. The use of synthetic models, as explored in this research, can approximate results effectively. Therefore, further investigation into the algorithm's performance with the use of comprehensive real field data and laboratory analysis is crucial. Conducting detailed studies that incorporate actual reservoir conditions and fluid properties can offer invaluable insights. These investigations can help validate the algorithm's performance under real-world scenarios and guide refinements to make it more robust and adaptable.

An improved LSK algorithm was introduced in the study [8]. This algorithm is accurate when dealing with zero binary interaction parameters (BIPs). For cases involving non-zero BIPs, an approximation technique known as regression was employed. When applying an equation of state with non-zero binary interaction coefficients, the authors proposed an innovative analytical solution. To decrease the number of independent variables, they redesigned the EOS parameters and used the reduction approach, which can handle non-zero BIPs precisely.

As a result of their effort, they developed a new set of variables and factors that they used to build the fugacity coefficients (reduction parameters). Since it can precisely handle scenarios with non-zero BIPs, the analytical reduction-based delumping approach consistently outperforms the earlier regression-based delumping method.

A comparison between the analytical delumping [7] and LSK delumping [5] was carried out in the context of reservoir simulation results in [8]. The study concluded that analytical delumping provides better results with high accuracy than LSK delumping.

The equations for the delumping procedure were provided by the research [9], which then used an example involving a North Sea reservoir fluid description and a CVD experiment to validate them. To evaluate the LSK delumping, they applied the delumping methods developed in the papers [4, 5]. They observed that both processes were performing quite well when they compared the results of delumping to those from the flash of the whole system. It was found [5] that delumping method's outcomes for K-values were only slightly impacted by heavy components and a small number of pseudo-components.

To study how fluid behaves during production, the scientists used a continuous volume depletion experiment. They noticed that the delumped and complete systems' vapor fractions have only a small deviation of 0.006 and concluded that the results of the delumping are quite accurate. In comparison to non-hydrocarbon compounds, hydrocarbon compound variances were smaller.

Fifth SPE comparison solution project additionally investigated the accuracy of the delumping approach with five lumping schemes. Six components, including N_2 and CO_2, as well as non-hydrocarbons, were determined through a lumping technique. The fluid descriptions received after delumping were equivalent to the fluid descriptions obtained from the reservoir simulation with the non-lumped system according to the experiment's results. The delumping approach can be used to link the upstream and downstream forecasts since it produced reliable outcomes when applied to the data from a reservoir simulation [9]. Notably, the precision of the delumping in the study is limited by the precision of the lumping procedure. In essence, the effectiveness of the delumping procedure hinges on the ability to properly and consistently lump components into appropriate groups. Thus, it is important to reconsider and refine the delumping technique with a focus on reducing sensitivity to lumping errors.

In a study conducted by the research group [6], the efficiency and accuracy of the LBW delumping approach were demonstrated using two test cases: the depletion of a volatile oil reservoir and gas injection processes. All the BIPs were set to zero in both scenarios. They used the lumped fluid model, which consisted of 7 components and the detailed fluid model of 16 components in the first example. The production profiles were almost identical. They deduced that a lumped model works well for simulating fluid phase behavior. The delumping approach was then applied to the outcomes of the lumped fluid simulation. The predicted proportions of the various detailed components in the lumped component correspond to the results of the detailed fluid simulation. The outcomes were of the highest accuracy degree.

For the gas injection procedure, a reservoir simulation was initially conducted using a precise fluid model, and then the operation was repeated using a lumped system. The gathered results revealed that the seven-component model was once again suitable for simulating the fluid's phase behavior under reservoir conditions.

The third example was a rerun of the first experiment with non-zero BIPs included in the EOS. Better agreements were found in the first two situations. For heavier components, as opposed to light ones, the agreement was essentially accurate. The accuracy of the approach is significantly decreased when nonzero BICs are present, but the results are still satisfactory [6]. These observations emphasize the ongoing need for research in this field, as there are complexities and unresolved issues associated with the inclusion of BICs in compositional reservoir simulations. Further investigations may shed light on ways to improve the accuracy and reliability of such simulations, ensuring their practicality and effectiveness.

An implementation of the LBW delumping approach was detailed in a publication by researchers [10] using the example of a real Middle Eastern gas condensate reservoir. The lack of binary interaction coefficients (BIPs) for the lumped or detailed fluid EOS and the use of a thorough lumping process can both contribute to the results' high accuracy. The accuracy of the LBW approach is slightly reduced by non-zero BIPs, according to prior research by [5].

Although the "detailed" EOS model was largely calibrated to data suitable for surface calculations, its accuracy under reservoir conditions was not as good as it could be. They decided to test the delumping method's accuracy on a tiny "quality control" issue before using it on the entire reservoir model. For the simulations of compositional reservoirs, the scientists developed two EOS models: a "lumped" EOS model, which consisted of 8 components and a "detailed" one of 16 components.

To maintain consistency between the lumped and detailed fluid descriptions, they concluded that greater attention must be paid to the development of the EOS models. Using the technique as a postprocessor rather than inside the reservoir simulator would be another enhancement. The reservoir simulation results would not be affected by this, but it would save from keeping a very big output file. The outcomes raised confidence in the quality of the surface facility design [10]. However, it's crucial to acknowledge the actual presence of both underscoring and overscoring in the results, stemming from the unforeseen conditions and complexities related to non-zero BIPs. These complexities underscore the ongoing need for further research in this domain, aiming to develop more robust and practical techniques for fluid composition modeling.

In summary, the research on delumping techniques in petroleum engineering has advanced significantly over the years. Various methods, such as the LSK algorithm and LBW approach, have been developed to address the challenges of simplifying fluid compositions for reservoir simulation. These methods have shown promise in improving accuracy and efficiency. However, there are still several shortcomings in the existing research. These include limitations in handling non-zero binary interaction parameters (BIPs), a heavy reliance on simplified fluid models with a limited number of components, and a lack of comprehensive validation using real field data.

Furthermore, the delumping procedure should be applied with a reduction approach rather than a regression approach. The regression method has limitations, especially at low BIP values, and gives less efficient results. Using a reduction method based on accurate calculations of equilibrium constants (K-values) and a calibrated equation of state, it becomes possible to obtain a detailed fluid description. Moreover, uncertainty quantification and broader applicability to different reservoir types and conditions need further attention.

An option to overcome the relevant difficulties can be outlined in the approach discussed in the study [7], in handling cases with non-zero binary interaction parameters (BIP). This suggests that this approach, compared to LSK and analytical variance removal methods, consistently produces better results in the study as reported in [5] and analytical variance removal methods, consistently produces better results in the study [8]. This analytical mixing removal method has been successfully tested in complex cases involving various reservoir fluids and reservoir processes.

Regarding Kazakhstan, which has large fields such as Karachaganak, Kashagan and Tengiz, where sour gas injection continues, obtaining a detailed fluid description is critical for compositional modeling. The consideration of BIP in the phase equilibrium equations allows the calibration of shortcomings and improves the accuracy of phase equilibrium models for multicomponent mixtures.

All this allows us to argue that it is important to conduct a study devoted to further investigating and improving delumping techniques for fluid characterization, particularly in the context of handling non-zero binary interaction parameters (BIPs) and enhancing the accuracy and efficiency of reservoir simulations for complex multicomponent mixtures.

3. The aim and objectives of the study

The aim of the study is to conduct a comprehensive fluid description through the implementation of a modified delumping procedure. This procedure will be employed to process the results obtained from compositional reservoir modeling, with the ultimate aim of enhancing the planning and modeling of surface facilities for oil extracted from the Caspian basin. Additionally, the study seeks to demonstrate that delumping can serve as a viable alternative to traditional laboratory analysis for fluid characterization.

To achieve this aim, the following objectives are accomplished:

– to conduct laboratory experiments, including flash liberation test, constant mass expansion test for fluid characterization of the Caspian basin oil;

– to group components higher than heptane plus fraction based on the principles of the Gamma Distribution Model;

– to delump compositional modeling results;

– to model fluid change in PVTsim according to PVT change;

– to compare numerical and simulation of PVTsim results to laboratory experiments.

4. Materials and methods

4. 1. Object and hypothesis of the study

The object of the study is detailed fluid compositions.

The subject of the study is addressing the challenges of accurately characterizing detailed fluid compositions in the context of compositional reservoir modeling.

This procedure is intended to connect reservoir modeling with surface facility modeling, enhancing the overall planning and modeling efficiency for onshore oil production facilities, specifically focusing on Caspian oil.

To support the research objectives, several key assumptions have been made.

Firstly, the consistency assumption is fundamental, relying on the conservation of mass balance between the delumped and lumped mixtures. Additionally, the research assumes the homogeneity of properties, implying that the mole fractions of individual components in each phase remain nearly identical for both the detailed and lumped mixtures.

Moreover, the equality of reduction parameters is a crucial assumption, where the reduction parameter for the lumped system is considered equal to the sum of the prod-

ucts of the individual components' mole fractions and their corresponding reduction parameters for the detailed system. These assumptions lay the foundation for the research's methodology.

Additionally, there is a specific restriction on binary interaction parameters (BIPs), which is that all BIPs for components within the same group must be zero. This simplification highlights that interactions between components within the same group are assumed to be negligible in the model.

In the laboratory phase of the research, a bottom-hole sample of reservoir fluid was taken at field X in the Caspian basin. This sample was subsequently sent to the laboratory of "Weatherford-CER" LLP in Aktau for PVT research, with detailed information provided in Table 1.

Table 1

General information of oil sample

Oil field	**X**
Perforation interval	610–617 m
Selection point	600 m
Sample type	bottom-hole oil sample
Reservoir pressure	53.83 kgf/cm^2
Reservoir temperature	30.22 °C

Opening pressures were measured on a depth sample container. Sample validation was confirmed by determining the saturation pressure in the PVT cell at reservoir temperature. The results of the sample validation are shown in Table 2.

Table 2

Validation of bottom-hole oil sample

Bottom-hole oil sample							
Reservoir conditions		Container opening		Water content	Sample volume P=141 kg/cm^2	Saturation pressure	
P_{res}, kg/cm^2	T_{res}, °C	P, kg/cm^2	T, °C	cm^3	cm^3	P_{sat}, kg/cm^2	T_{res}, °C
53.83	30.22	127.6	22	0	595	1.16	30.22

The following series of laboratory experiments were carried out to obtain the physico-chemical properties of reservoir oil:

1. Flash Liberation Test.
2. Constant Mass Expansion (CME).

4. 2. Flash Liberation Test

The PVT cell was heated to reservoir temperature and approximately 50 cm^3 of reservoir fluid was transferred to the PVT cell. After transferring the sample, the reservoir fluid from reservoir conditions in a single-phase state was degassed to standard surface conditions to calculate the reservoir volume factor (B_o), gas factor and surface fluid density. The results are shown in Tables 3–5 – main results for oil sample from field X.

Tables 3–5 demonstrate basic fluid properties such as oil formation volume factor, shrinkage factor, oil density. It can be seen that approximately 7.09 % of 1 m^3 of gas dissolved in oil under reservoir conditions. The formation volume factor suggests that the volume of oil increases slightly (by a factor of 1.0053) when it moves from reservoir conditions to standard conditions.

Table 3

Flash Liberation Test results

Pressure, kg/cm^2		Oil FVF B_{od}	R_{sd}, cm^3/cm^3	Oil density, g/cm^3
P_{test}	140.6	0.9936	0.0642	0.8235
	70.3	0.9999	0.0642	0.8184
P_{res}	53.8	1.0015	0.0642	0.8171
	42.18	1.0027	0.0642	0.8162
	28.12	1.0041	0.0642	0.815
	14.06	1.0057	0.0642	0.8138
	7.03	1.0064	0.0642	0.8132
	5.27	1.0066	0.0642	0.813
	3.52	1.0068	0.0642	0.8129
	1.76	1.007	0.0642	0.8127
	1.65	1.007	0.0642	0.8127
	1.41	1.0071	0.0642	0.8127
	1.34	1.0071	0.0642	0.8127
	1.27	1.0069	0.0642	0.8127

Table 4

Flash Liberation Test results

P_{sat}, kg/cm^2	Oil FVF B_{od}	R_{sd}, cm^3/cm^3	Gas FVF B_g	Oil density, g/cm^3	Z-factor gas	Gravity air=1
1.12	1.006941	0.0457	0.9506	0.8126812	0.99805	1.1860
1.09	1.006930	0.0282	0.9814	0.8126822	0.99803	1.1930
1.05	1.006918	0.0106	1.0142	0.8126833	0.99801	1.2004
1.03	1.006911	0.0000	1.0349	0.8126839	0.99800	1.2051

Table 5

Flash Liberation Test results

Reservoir conditions		Units
Gas factor	0.0824	m^3/m^3
Relative gas density (air=1.000)	1.1609	–
FVF (B_o)	1.0053	–
Oil shrinkage coefficient	0.5263	%
Solution gas-oil ratio	0.0709	m^3/m^3
Standard conditions		
Oil density	0.8183	g/cm^3
Water content	<0.01	%

4. 3. Constant Mass Expansion (CME)

Calculation results are compared with a constant mass expansion experiment (CME). A defined volume of reservoir fluid was transferred to a PVT cell. The transferred fluid was stabilized in a single-phase state for 24 hours under reservoir conditions. Isothermal pressure reduction was carried out at least 10 pressure steps above saturation pressure. Below the saturation pressure, a similar pressure reduction was carried out to the maximum expansion of the PVT cell.

The saturation pressure was determined visually and graphically. The saturation pressure was determined at 87.64 atm. Relative volume, PV ratio, reservoir compressibility (Z-factor) and density were calculated and presented in Tables 6–8 – Constant Mass Expansion (CME) results and Table 9 – Main results for oil sample from field X.

It can be seen from Table 8 that despite being slightly compressible, the oil maintains relatively consistent density values across the range of pressures. This suggests that it is not highly compressible, and the changes in volume are relatively small compared to the initial volume.

Table 6

Constant Mass Expansion (CME) results

Pressure, kg/cm^2		Relative volume V/V_b	Density, g/cm^3
Test pressure	140.6	0.986845	0.823514
	70.31	0.992985	0.818421
Reservoir pressure	53.8	0.99456	0.817125
	42.18	0.995708	0.816184
	28.12	0.997134	0.815016
	14.06	0.998606	0.813815
	7.03	0.999361	0.8132
	5.27	0.999551	0.813045
	3.52	0.999743	0.812889
	1.76	0.999935	0.812733
	1.65	0.999946	0.812724
	1.41	0.999973	0.812702
	1.34	0.999981	0.812696
	1.27	0.999989	0.812689

Table 7

Constant Mass Expansion (CME) results

P_{sat}	Relative volume	Y function
1.1	1.006600	5.7142
1.1	1.015219	5.6643
1.0	1.022147	5.6241

Table 8

Compressibility factor

Test conditions	Pressure range, kg^2/cm		Average compressibility factor, cm^2/kg
	From	to	
P_{test}	140.61	140.61	8.240×10^{-5}
	70.31	53.83	9.454×10^{-5}
P_{res}	53.83	42.18	9.782×10^{-4}
	42.18	28.12	1.003×10^{-4}
	28.12	14.06	1.033×10^{-4}
	14.06	7.03	1.066×10^{-4}
P_{sat}	7.03	5.27	1.083×10^{-4}

Table 9

Main results for oil sample from field X

Test conditions		Units of measurement
Pressure	140.6	kgf/cm^2
Temperature	30.22	°C
Constant Mass Expansion (CME)		
Saturation pressure	1.16	kgf/cm^2
Compressibility of fluid at saturation pressure	0.0001083	cm^2/kg

4. 4. Mathematical formulation or analytical part

For reliable modeling of the phase behavior required to describe a hydrocarbon mixture, calculations of equations are often complicated by a large number of components. The most common problem is either the modeling of a hydrocarbon system, or a combination of many fractions, which in turn have been determined experimentally, when the only and most accessible experimental data for the C7+ fraction are specific gravity and molecular weight.

The word "grouping" or "pseudo-formation" denotes a decrease in the number of parts that are used in the calculation of reservoir fluids by capital. This reduction is achieved directly due to applying the concept of a pseudo-component. The pseudo-component establishes the category of the purest parts, which connected together also assume a single element with SCN.

The SCN groups in their composition contain hundreds of isomers with a similar number of carbon atoms and hence similar boiling points. It is impossible to determine the original value of the molecular weight, due to the uncertainty of the values of isomers, which in turn are present in each group of SCN.

For instance, components with a molecular mass of hydrocarbon groups MI-1 to MI falling within the boundaries of these molecular weight values are included in the *i*-th group of the MCN.

Modeling of a compositional model is possible after providing a scheme for grouping the SCN, which in turn acts as primary data. In terms of the oil composition of producing wells, the obtained results of the compositional model are investigated by removing uncertainties, which in turn provides an opportunity to investigate the model of phase behavior.

4. 5. Lumping the C_{7+} fraction procedure into 4 components

Gamma-distribution model: The three parameters gamma distribution model is used for describing molar distribution:

$$f(M)=\frac{(M-\tau)^{y-1}\exp\left(-\frac{(M-\tau)}{\beta}\right)}{\beta^{y}\Gamma(y)}, \quad (1)$$

where Γ – gamma function and β is given by:

$$\beta=\frac{M_{C_{7+}}-\tau}{y}. \quad (2)$$

The parameter τ is a minimum molecular weight of the C_{7+} tail.

The key parameter γ controls the shape of $f(M)$.

Change integration variables are given in Table 10:

$$\sum_{k=1}^{n}W_k^{(n)}z_{total}=z_{total}\sum_{k=1}^{n}W_k^{(n)}=z_{total}. \quad (3)$$

$$z_k=\sum_{k=1}^{n}W_k^{(n)}z_{total}. \quad (4)$$

$$M_k=\frac{M_{total}}{Z_{total}}\frac{1}{\Gamma(\gamma)}X^{\gamma-1}. \quad (5)$$

Table 10

Quadrature points

n=2	
X_1=0.5858	W_1=0.8536
X_2=0.34142	W_2=0.1464
n=3	
X_1=0.4158	W_1=0.7111
X_2=2.2943	W_2=0.2785
X_3=6.2960	W_3=0.0104
n=4	
X_1=0.3226	W_1=0.6032
X_2=4.5366	W_2=0.3574
X_3=6.2960	W_3= 0.0384
X_4=9.3951	W_4=0.0005

The range of γ is usually from 0.5 to 2.5. To determine γ, the C_{7+} tail is constructed and density distribution curves with different values of γ are drawn in order to find the best match with the shape of C_{7+}. Fig. 1 represents the Mole fraction vs. Molar weight Plot according to γ *distribution*.

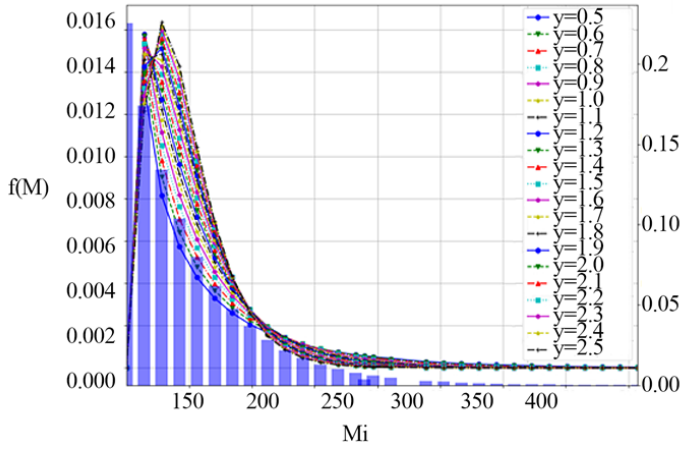

Fig. 1. Mole fraction vs. Molar weight Plot

Fig. 1 demonstrates that the best fit was achieved with γ=0.5, which was then used for lumping pseudo-components.

4. 6. Delumping the C_{7+} fraction procedure

The procedure that is based on the reduction concept is called the ungrouping procedure. It is analytical and consistent, and it considers non-zero binary interaction parameters in three-dimensional equations of state. This technique is aimed at identifying, by designing information on the molar fractions of components, equilibrium coefficients, and molar fractions of phases, based on available data of the classified system of a component.

The general form of two-parameter cubic EoS is used:

$$P=\frac{RT}{v-b}-\frac{a}{(v+\delta_1 b)\times(v+\delta_2 b)}, \tag{6}$$

where:

$$\delta_1=1+\sqrt{2}, \tag{7}$$

and:

$$\delta_2=1-\sqrt{2}. \tag{8}$$

The implicit form of the EoS can be written as:

$$Z^3+\left[(\delta_1+\delta_2-1)B-1\right]Z^2+ \\ +\left[A+\delta_1\delta_2 B-(\delta_1+\delta_2)B(B+1)\right]Z- \\ -\left[AB+\delta_1\delta_2 B^2(B+1)\right]=0. \tag{9}$$

The van der Waals one-fluid mixing rules are used where *A* (energy) and *B* (volume) parameters can be found by:

$$A=\sum_{i=2}^{nc}\sum_{j=1}^{nc}y_i y_j A_{ij}, \tag{10}$$

$$B=\sum_{i=1}^{nc}y_j B_j. \tag{11}$$

For flash calculations, the set of reduction parameters is used:

$$A=a^2+2\sum_{k=1}^{m}\theta_k y_k+\sum_{k=1}^{m}\theta^2, \tag{12}$$

where:

$$\alpha=\sum_{j=m+1}^{nc}y_j\alpha_j. \tag{13}$$

$$\theta=\alpha_k y_k. \tag{14}$$

$$y_k=\sum_{i=k+11}^{nc}y_i y_{ki}. \tag{15}$$

$$k=1,m.$$

$$y_{ki}=\alpha(1-C_{ki}). \tag{16}$$

Ψ_i in terms of the reduction parameters is calculated by:

$$\psi=\sum_{j=1}^{m}x_j^{(i)}\theta_j y_{ji}+a_j\lambda^{(i)};\ \ i=1,nc. \tag{17}$$

The compressibility factor, which depends on *A* and *B*, hence *Z*=*Z*(*p*, *T*, *Q*):

$$Z^3+\left[(\delta_1+\delta_2-1)B-1\right]Z^2+ \\ +\left[a^2+2\sum_{k=1}^{m}\theta_k+\delta_1\delta_2 B^2-(\delta_1+\delta_2)B(B+1)\right]Z- \\ -\left[B\left(a^2+2\sum_{k=1}^{m}\theta_k y_k+\sum_{k=1}^{m}\theta_k\right)+\delta_1\delta_2 B^2(B+1)\right]=0. \tag{18}$$

The vector of the reduction parameters *Q* is given by:

$$y_i=K_i x_i=\frac{z_i K_i}{1+V(K_i-1)}. \tag{19}$$

The fugacity equation is expressed below:

$$\ln\varphi_{ip}(Q_p)=h_{op}(Q_p)+h_{ap}(Q_p)\alpha_i+ \\ +h_{Bp}(Q_p)B_i+\sum_{k-1}^{m}h_{ykp}(Q_p)\gamma_{ki}, \tag{20}$$

$$i=1,nc, \tag{21}$$

$$p=L,V, \tag{22}$$

where:

$$h_o(Q)=-\ln(Z-B), \tag{23}$$

$$h_a(Q)=\frac{-2\lambda^{iL}}{\triangle B}\ln E, \tag{24}$$

$$h_B(Q)=\frac{Z-1}{B}-h_a(Q)\frac{a^2+2\sum_{k=1}^{m}\theta_k y_k+\sum_{k=1}^{m}\theta_k}{2B\theta\lambda^{(i)}}, \tag{25}$$

$$h_{yk}(Q)=\frac{-x_k^{(i)}\theta_k}{\lambda^{(i)}}h_a(Q), \tag{26}$$

$k=1,m.$

Furthermore, pressure, temperature, and reduction parameters are the functions of the fugacity equation.

For the system with non-zero binary interaction parameters, the ungrouping equation can be expressed as:

$$\ln K_i\left(Q_L,Q_V\right)=\Delta h_0\left(Q_L,Q_V\right)+{}_\Delta h_\alpha\left(Q_L,Q_V\right)\alpha_i+$$
$$+{}_\Delta h_B\left(Q_L,Q_V\right)B_i+\sum_{k-1}^{m}{}_\Delta h_{yk}\left(Q_L,Q_V\right)y_{ki}. \quad (27)$$

The information of lumped composition is used to estimate all values of the reduction parameter functions. Also, parameters of the comprehensive composition of the fluid are components of the reduction matrix, such as the reduction coefficients, parameters of EOS.

Mainly, the ln(K)-values are expressed as a sum of consequences with the first factor depending only on reduction parameters, and the second factor depending particularly on component properties.

The ungrouping equation ln(K_i) relates the equilibrium relation of the complex solution to the consequences of flash calculations for a lumped fluid and extends to systems with nonzero binary interaction parameters.

Newton-Raphson equation, which is based on the equation of equilibrium constant of the comprehensive system, allows estimating the molar fraction of vapor:

$$\sum_{i=1}^{nc}\left(y_i-x_i\right)=\sum_{i=1}^{nc}\frac{z_i\left(K_i-1\right)}{1+V\left(K_i-1\right)}. \quad (28)$$

Overall, the delumping algorithm can be summarized as follows:

1. The lumped pseudo-components are flashed (at given T and p).

2. The obtained information from the lumped system is used for $dh(Q)$ functions calculation.

3. Using (3), the K values for the detailed mixture are calculated.

4. The component mole fractions are computed for liquid and vapor equilibrium phases [4].

5. Results of comprehensive fluid description through the implementation of a modified delumping procedure

5. 1. Results of the experimental analysis

An oil sample from the bottom hole of oil field X was obtained, and the fluid composition information was derived from a crude oil test tube. The separation process involves volatile components using an inert gas (carrier phase) flowing through a stationary phase with a large surface area. It's important to note that the stationary phase and the substances to be separated do not react with the carrier gas. The separation process is based on differences in the volatility and solubility (or adsorbability) of the mixture's components. The gas chromatograph comprises a sample input mechanism, a column, and a flame ionization detector. The detector signal is integrated and accumulated using either a traditional integrator or a computer-based chromatographic data processing system. Calibration of the gas chromatograph is achieved using a mixture of C6 to C36 hydrocarbons as an external standard. The relevant findings, including component composition according to PVT analysis, are presented in Table 11.

Table 11

Component composition of reservoir fluid according to PVT laboratory analysis

Component		Liberated gas	Stabilized oil		Reservoir fluid	
		weight, %	mole, %	weight, %	mole, %	weight, %
Nitrogen	N_2	84.835	0.000	0.000	0.120	0.019
Carbon dioxide	CO_2	0.566	0.000	0.000	0.001	0.000
Hydrogen sulfide	H_2S	0.000	0.000	0.000	0.000	0.000
Methane	C_1	0.253	0.000	0.000	0.000	0.000
Ethane	C_2	0.101	0.000	0.000	0.000	0.000
Propane	C_3	1.296	0.000	0.000	0.002	0.000
Isobutane	i-C_4	3.227	2.287	0.754	2.288	0.755
Butane	n-C_4	3.244	0.000	0.000	0.005	0.002
Isopentane	i-C_5	2.002	3.104	1.270	3.103	1.271
Pentane	n-C_5	1.938	2.601	1.064	2.600	1.065
Hexane	C_6	0.843	4.500	2.199	4.495	2.199
Heptane	C_7	1.622	9.924	5.639	9.912	5.639
Octane	C_8	0.055	15.004	9.719	14.982	9.716
Nonane	C_9	0.003	7.537	5.482	7.527	5.481
Dean	C_{10}	0.013	6.954	5.611	6.945	5.610
Undecane	C_{11}	0.003	5.749	4.792	5.741	4.791
Dodecane	C_{12}	0.000	4.848	4.426	4.841	4.425
Tridecane	C_{13}	0	4.452	4.418	4.446	4.417
Tetradecane	C_{14}	0	3.770	4.062	3.765	4.061
Pentadecane	C_{15}	0	3.953	4.617	3.947	4.616
Hexadecane	C_{16}	0	3.102	3.905	3.098	3.904
Heptadecane	C_{17}	0	2.682	3.605	2.678	3.604
Octadecane	C_{18}	0	2.496	3.553	2.493	3.552
Nonadecane	C_{19}	0	2.135	3.184	2.132	3.184
Icosane	C_{20}	0	1.837	2.864	1.834	2.863
Heneicosane	C_{21}	0	1.617	2.669	1.615	2.668
Docosane	C_{22}	0	1.391	2.406	1.389	2.405
Triclosan	C_{23}	0	1.233	2.224	1.232	2.223
Tetracosane	C_{24}	0	1.025	1.924	1.024	1.924
Pentacosane	C_{25}	0	0.926	1.811	0.924	1.810
Hexacosane	C_{26}	0	0.798	1.624	0.797	1.624
Heptacosane	C_{27}	0	0.715	1.517	0.714	1.517
Octacosane	C_{28}	0	0.621	1.366	0.620	1.365
Nonacosane	C_{29}	0	0.606	1.381	0.605	1.381
Triacontane	C_{30}	0	0.478	1.127	0.477	1.127
Hentriacontane	C_{31}	0	0.446	1.088	0.445	1.087
Dotriacontane	C_{32}	0	0.369	0.928	0.368	0.928
Tritriacontane	C_{33}	0	0.343	0.892	0.343	0.892
Tetratriacontane	C_{34}	0	0.251	0.672	0.251	0.672
Pentatriacontane	C_{35}	0	0.242	0.667	0.242	0.667
Hexatriacontane plus	C_{36+}	0	2.002	6.537	1.999	6.535
Balance	–	100.000	100.000	100.000	100.000	100.000

Table 11 represents the component composition of the liberated gas, reservoir oil and stabilized oil, both in mole fractions and weight fractions, ranging from nitrogen (N_2) to heavy hydrocarbons (C_{36+}). The liberated gas is primarily composed of nitrogen (N_2) at approximately 84.835 % in both weight and mole percentages. Nitrogen is the dominant component, representing the largest fraction of the liberated gas. Other minor components in the liberated gas include carbon dioxide (CO_2), methane (C_1), ethane (C_2), propane (C_3), isobutane (i-C_4), butane (n-C_4), isopentane (i-C_5), pentane (n-C_5), hexane (C_6),

heptane (C_7), and octane (C_8), each contributing to the composition in varying amounts. Heavier hydrocarbons from nonane (C_9) to hexatriacontane plus (C_{36+}) are also present in trace amounts in the liberated gas, with increasing carbon numbers. Notably, the stabilized oil does not contain lighter hydrocarbons such as methane (C_1) or ethane (C_2). The reservoir fluid has a similar composition to the stabilized oil, with heavier hydrocarbons dominating the composition, ranging from isobutane (i-C_4) to hexatriacontane plus (C_{36+}). Just like in the stabilized oil, the reservoir fluid does not contain significant quantities of lighter hydrocarbons such as methane (C_1) or ethane (C_2). The absence or very low presence of light hydrocarbons such as methane (C_1) and ethane (C_2) in both weight and mole percentages indicates that the oil is not characterized by these lighter, more volatile components. The significant presence of hydrocarbons with carbon numbers ranging from nonane (C_9) to hexatriacontane plus (C_{36+}) suggests that the oil is rich in heavier, long-chain hydrocarbons.

5. 2. Results of the numerical approach

The physicochemical properties were determined as the input parameters for further formulas. Since the laboratory tests were conducted at atmospheric pressure, the calculation process employed a pressure and temperature of 0.1 MPa and 303.37 K, respectively.

Normal alkanes from methane (C_1) to hexatriacontane plus (C_{36+}) make up the reservoir mixture that is in contact with carbon dioxide and nitrogen, two non-hydrocarbon substances with relatively high hydrocarbon component ratios. To make the calculation of component properties, consistency is very important. The EoS parameters are the same for both groups lumped and detailed fluid. The algorithm of delumping is based on the assumption that 'a' and 'b' parameters of the EoS are equal throughout the entire calculation process. This step ensures the reliability of results and its high accuracy. Table 12 presents the composition and component properties of the reservoir oil.

Table 12

Composition, component properties and BIPs for the detailed mixture

Component		T_c, K	P_c, bar	Acentric Factor ω	C CO_2-J	C N_2-J
Nitrogen	N_2	126.2	33.94	0.04	0.001482469	0
Carbon dioxide	CO_2	304.2	73.76	0.225	0	0.001482469
Hydrogen sulfide	H_2S	497.402	1.991	0.2852	0.000500266	0.000260939
Methane	C_1	576.105	1.949	0.0675	0.009224393	0.003341736
Ethane	C_2	628.818	1.92	0.1989	0.001082479	3.14796E-05
Propane	C_3	670.658	1.898	0.152	3.0062E-08	0.001495825
Isobutane	i-C_4	670.658	1.898	0.176	0.000608985	0.003982309
Butane	n-C_4	706.225	1.878	0.193	0.000608985	0.003982309
Isopentane	i-C_5	706.225	1.878	0.227	0.001949714	0.00680349
Pentane	n-C_5	737.613	1.862	0.251	0.001949714	0.00680349
Hexane	C_6	765.976	1.846	0.296	0.003631454	0.009698141
Heptane	C_7	792.026	1.833	0.3374	0.004903798	0.011699881
Octane	C_8	816.237	1.82	0.3743	0.006362749	0.013881136
Nonane	C_9	838.943	1.808	0.4205	0.008213005	0.016529983
Dean	C_{10}	860.389	1.796	0.4824	0.009879978	0.018836488
Undecane	C_{11}	880.761	1.785	0.4826	0.011466312	0.020978473
Dodecane	C_{12}	900.205	1.775	0.57	0.013051527	0.023077741
Tridecane	C_{13}	918.836	1.765	0.5705	0.014516185	0.024986963
Tetradecane	C_{14}	936.747	1.755	0.66	0.015732782	0.026553774
Pentadecane	C_{15}	954.016	1.746	0.6605	0.017194421	0.028416143
Hexadecane	C_{16}	970.708	1.737	0.75	0.018172472	0.029651387
Heptadecane	C_{17}	986.876	1.728	0.7505	0.019107486	0.030824792
Octadecane	C_{18}	1002.57	1.72	0.828	0.019707525	0.031574208
Nonadecane	C_{19}	1017.82	1.711	0.8299	0.020093274	0.032054567
Icosane	C_{20}	1032.68	1.703	0.9134	0.020360969	0.032387282
Heneicosane	C_{21}	1047.16	1.695	0.9145	0.020537638	0.032606584
Docosane	C_{22}	1061.3	1.687	0.9154	0.0205256	0.032591649
Triclosan	C_{23}	1075.12	1.679	1.0355	0.020377209	0.03240745
Tetracosane	C_{24}	1088.64	1.671	1.0365	0.020098414	0.032060959
Pentacosane	C_{25}	1101.88	1.664	1.0375	0.019654135	0.031507636
Hexacosane	C_{26}	1114.86	1.656	1.0385	0.019062249	0.030768182
Heptacosane	C_{27}	1127.59	1.648	1.0395	0.018266207	0.029769341
Octacosane	C_{28}	1140.08	1.641	1.1814	0.017373912	0.028643461
Nonacosane	C_{29}	1152.36	1.634	1.1824	0.016339376	0.027329183
Triacontane	C_{30}	1164.43	1.626	1.1834	0.015164264	0.025823605
Hentriacontane	C_{31}	1176.3	1.619	1.1844	0.013852635	0.024125314
Dotriacontane	C_{32}	1187.97	1.612	1.185	0.012408885	0.022231159
Tritriacontane	C_{33}	1199.48	1.604	1.1854	0.010840641	0.020139053
Tetratriacontane	C_{34}	1210.8	1.597	1.1513	0.009160367	0.017848633
Pentatriacontane	C_{35}	1221.97	1.59	1.1515	0.007388789	0.015363407
Hexatriacontane plus	C_{36+}	1221.97	9.29	1.1519	0.009178738	0.003314076

The critical properties, acentric factor, and Joule-Thomson coefficients were calculated for each component. Nitrogen has a relatively low critical temperature of 126.2 K, indicating that it can be easily liquefied at relatively low temperatures and pressures. In contrast, heavier hydrocarbons have much higher critical temperatures. Critical pressures also show significant variation. Carbon dioxide has a relatively high critical pressure of 73.76 bar, indicating that it requires high pressure to liquefy even at its relatively high critical temperature. In contrast, gases like hydrogen sulfide and methane have much lower critical pressures, making them easier to liquefy under lower pressures. Furthermore, the obtained critical parameters were utilized for calculating temperature-dependent parameters.

5. 3. Results obtained from the lumping algorithms

The components from C_7 through C_{36+} are divided into four distinct groups. According to Leibovici based on the detailed component parameters data, the critical temperature, pressure, acentric factor and BIPs were calculated for pseudo-components. The composition and properties of the grouped components are assigned and organized in Tables 13, 14.

Table 13

Component composition of lumped fluid

Component	Mole, %	Mole weight
N_2	0.12	28.014
CO_2	1.00E-03	44.01
C_3	0.002	44.097
iC_4	2.283	58.124
nC_4	0.005	58.124
iC_5	3.096	72.151
nC_5	2.594	72.151
C_6	4.485	86.178
C_7–C_{11}	45.007	190.86
C_{12}–C_{19}	27.339	264.35
C_{20}–C_{29}	10.73	375.15
C_{30}–C_{80}	4.337	508.438
Balance	100	–

Table 14 demonstrates the calculation of critical parameters, acentric factor, and Joule-Thomson Coefficients for grouped components.

5. 4. Results from PVTsim software

Fig. 2 shows the phase envelopes of the lumped and detailed mixtures. As observed in Fig. 2, there is an excellent agreement between the phase boundaries of the detailed and lumped mixtures for bubble points, with some acceptable discrepancies for dew points.

The lumped pseudo-components are flashed at 0.1 MPa and 303.37 K. The results are presented in Tables 15–19 and are used to obtain reduction parameters for equilibrium constants equations. For low BIPs values, the deviations of the results are not so noticeable, that is why the approach [5] can also be used. However, with an increase in the mole fraction of a component, the BIP also increases. For this reason, for non-zero BIPs between pseudo-components, a new analytical delumping approach [7] must be utilized. This method is based on the range of the reduction variables, the number of which is much smaller than for the initial range of parameters.

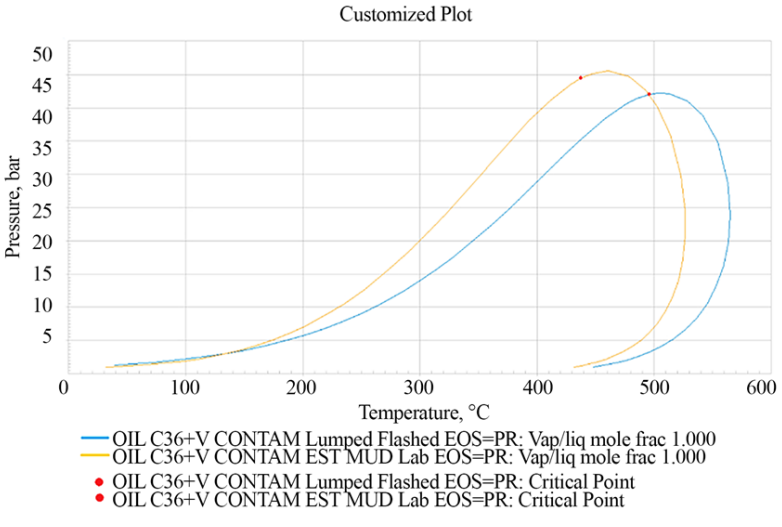

Fig. 2. Phase boundaries for the detailed and lumped mixtures from PVTsim

Table 14

Composition, component properties and BIPs for the lumped mixture

Component		T_c, K	P_c, bar	Acentric Factor	C CO_2-J	C N_2-J
Nitrogen	N_2	126.2	33.94	0.04	0	0
Carbon dioxide	CO_2	304.2	73.76	0.225	0	–0.017
Hydrogen sulfide	C_1	190.6	46	0.008	0.12	0.0311
Methane	C_2	305.4	48.84	0.098	0.12	0.0515
Ethane	C_3	369.8	42.46	0.152	0.12	0.0852
Propane	iC_4	408.1	36.48	0.176	0.12	0.1033
Isobutane	nC_4	425.2	38	0.193	0.12	0.08
Butane	iC_5	460.4	33.84	0.227	0.12	0.0922
Isopentane	nC_5	469.6	33.74	0.251	0.12	0.1
Pentane	C_6	507.4	29.69	0.296	0.12	0.08
PC-1	C_{7+}	576.588	25.72	0.4129	0.1	0.08
PC-2	C_{12+}	694.648	17.73	0.6844	0.1	0.08
PC-3	C_{20+}	828.626	14.37	1.0132	0.1	0.08
PC-4	C_{30+}	1043.03	12.43	1.1691	0.1	0.08

$\ln(K_i)$ is stated as a sum of products where the first factor depends solely on the reduction parameters and the second one only on the properties of an individual component. All the calculations are done by assuming that there are only liquid and vapor phases of the mixture. The natural logarithm of fugacity is presented by the $\ln(\varphi)$ "fi" term. This value is negative, and the values of the vapor-liquid equilibrium phases (Ki) range from 1.4 to 0.0005 and decrease with the amount of carbon atoms, potentially expanding the liquid phase. Fig. 3 displays crossplots of $\ln K$ of the delumped mixture vs. $\ln(K)$ of the initial mixture (R^2=0.9897). The suggested technique yields excellent agreement for K values and mole fractions. As expected, there is a linear relationship (y=x) between the equilibrium constants for the initial and ungrouped systems.

Using these equilibrium constants, the information of the detailed fluid is retrieved. The delumping of composite modeling results is presented in Table 17. The final composition data of the retrieved fluid was obtained through analytical methods and with the assistance of reservoir simulation software such as PVTsim, allowing for a comprehensive comparison of the results (Tables 20, 21).

Table 15

Reduction parameters of liquid and vapor phases

Liquid phase		Vapor phase	
z_L – mole fraction of a component in the liquid phase	0.845269546	z_V – mole fraction of a component in the vapor phase	0.975248222
– energy parameter for the liquid phase	1.025255749	E_V – energy parameter for the vapor phase	1.010803559
$\lambda_L^{(i)}$ – coefficient in (15)	8.168939953	$\lambda_V^{(i)}$ – coefficient in (15)	1.781657081
θ_{kL} – reduction parameter of the liquid phase	1.63293201	θ_{kV} – reduction parameter of the vapor phase	1.115901763
A_L – energy parameter EOS	0.128455215	A_V – energy parameter EOS	0.02801626
B_L – volume parameter EOS	0.007519815	B_V – volume parameter EOS	0.003719208
h_{0L} – function of reduction parameter in the liquid phase, eq. (23)–(26)	0.177035873	h_{0V} – function of reduction parameter in the vapor phase, eq. (23)–(26)	–0.028884145
$h_{\alpha L}$ – function of reduction parameter in the liquid phase	19.15915892	$h_{\alpha V}$ – function of reduction parameter in the vapor phase	3.639905008
h_{BL} – function of reduction parameter in the liquid phase	–40.60841086	h_{BV} – function of reduction parameter in the vapor phase	–51.20962804
$h_{\gamma kL}$ – function of reduction parameter in the liquid phase	3.829824195	$h_{\gamma V}$ – function of reduction parameter in the vapor phase	2.27977452
Δh_0 – function of reduction parameter in eq. (23)–(26)		0.205920019	
Δh_α – function of reduction parameter in eq. (23)–(26)		15.51925391	
Δh_B – function of reduction parameter in eq. (23)–(26)		10.60121718	
$\Delta h_{\gamma k}$ – function of reduction parameter in eq. (23)–(26)		1.550049676	

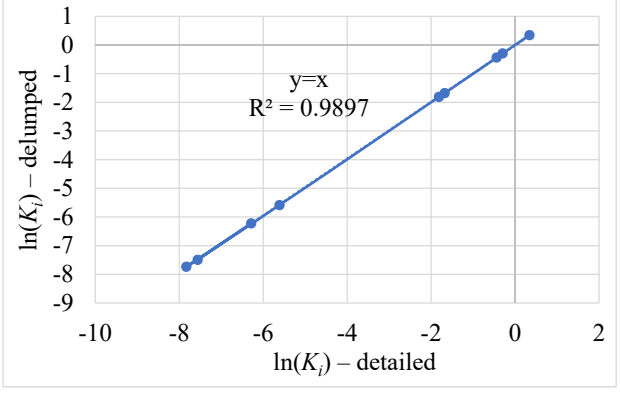

Fig. 3. Crossplot of ln(K) for example (reduction)

Table 16

Equilibrium constants calculation

Component	*ai*	*Bi*	*yki*	ln(*k*)
iC_4	0.0011	3.64802E-05	0.0773	0.3446
iC_5	0.0018	4.51285E-05	–0.4332	–0.438
nC_5	0.0018	4.51285E-05	–0.3411	–0.295
C_6	0.0025	5.41211E-05	–1.2405	–1.679
C_7	0.0032	6.06528E-05	–1.3321	–1.811
C_8	0.004	6.82103E-05	–3.7709	–5.584
C_9	0.0052	7.82054E-05	–5.168	–7.734
C_{10}	0.0065	8.78625E-05	–4.2081	–6.224
C_{11}	0.0079	9.78743E-05	–5.0399	–7.493

It can be seen from Table 21 that the results for the delumped components of PVTsim simulation match laboratory data.

Table 17

Flash of initial mixture

Component	*yi*	*xi*	*k*	ln(*k*)
iC_4	0.0323	0.0229	1.411	0.3443
iC_5	0.02	0.031	0.645	–0.439
nC_5	0.0194	0.026	0.7451	–0.294
C_6	0.0084	0.045	0.1873	–1.675
C_7	0.0162	0.0992	0.1634	–1.811
C_8	0.0006	0.15	0.0037	–5.609
C_9	3E–05	0.0754	0.0004	–7.829
C_{10}	0.0001	0.0695	0.0019	–6.282
C_{11}	3E–05	0.0575	0.0005	–7.558

Table 18

Flash of lumped mixture

Component	*yi*	*xi*	*k*	ln(*k*)
iC_4	0.0918	0.02283	4.0219	1.3918
nC_4	0.0001	0.00005	2.8	1.0296
iC_5	0.0345	0.03096	1.11434	0.1083
nC_5	0.0219	0.02716	0.80707	–0.214
C_6	0.0119	0.04485	0.26577	–1.325
C_7–C_{11}	0.0095	0.45007	0.02111	–3.858
C_{12}–C_{19}	1E–05	0.2734	3.7E–05	–10.22

Table 19

Flash of delumped mixture

Component	*yi*	*xi*	*k*	ln(*k*)
iC_4	0.0323	0.0229	1.4114	0.3446
iC_5	0.02	0.031	0.6452	–0.438
nC_5	0.0194	0.026	0.7445	–0.295
C_6	0.0084	0.0453	0.1866	–1.679
C_7	0.0162	0.0992	0.1636	–1.811
C_8	0.0006	0.15	0.0038	–5.584
C_9	3E–05	0.0754	0.0004	–7.734
C_{10}	0.0001	0.0695	0.002	–6.224
C_{11}	3E–05	0.0575	0.0006	–7.493

Table 20

Flash on delumped system (P=0.1 MPa, T=303.37 K). Analytical approach

Component		Total	Vapor	Liquid
		Mole, %	Mole, %	Mole, %
Nitrogen	N_2	0.12	84.823	0
Carbon dioxide	CO_2	0.001	0.57	0
Hydrogen sulfide	H_2S	0	0.000	0.000
Methane	C_1	0.005	0.2545	0.000
Ethane	C_2	0.001	0.1	0.000
Propane	C_3	0.002	1.2983	0.000
Isobutane	iC_4	2.283	3.2273	2.28653
Butane	nC_4	0.005	3.24232	0.000
Isopentane	iC_5	3.096	2.00268	3.10379
Pentane	nC_5	2.594	1.9377	2.60283
Hexane	C_6	4.485	0.84474	4.5273
Heptane	C_7	9.89	1.62281	9.92237
Octane	C_8	14.949	0.05637	15.0043
Nonane	C_9	7.51	0.0033	7.53676
Dean	C_{10}	6.93	0.01378	6.95368
Undecane	C_{11}	5.728	0.0032	5.74678
Dodecane	C_{12}	4.83	0	4.84779
Tridecane	C_{13}	4.436	0	4.43623
Tetradecane	C_{14}	3.757	0	3.75732
Pentadecane	C_{15}	3.938	0	3.938
Hexadecane	C_{16}	3.091	0	3.091
Heptadecane	C_{17}	2.672	0	2.672
Octadecane	C_{18}	2.487	0	2.488
Nonadecane	C_{19}	2.127	0	2.127
Icosane	C_{20}	1.83	0	1.83
Heneicosane	C_{21}	1.611	0	1.611
Docosane	C_{22}	1.386	0	1.386
Triclosan	C_{23}	1.229	0	1.229
Tetracosane	C_{24}	1.022	0	1.022
Pentacosane	C_{25}	0.922	0	0.922
Hexacosane	C_{26}	0.795	0	0.795
Heptacosane	C_{27}	0.712	0	0.712
Octacosane	C_{28}	0.619	0	0.619
Nonacosane	C_{29}	0.604	0	0.604
Triacontane	C_{30}	0.476	0	0.476
Hentriacontane	C_{31}	0.444	0	0.444
Dotriacontane	C_{32}	0.367	0	0.367
Tritriacontane	C_{33}	0.342	0	0.342
Tetratriacontane	C_{34}	0.25	0	0.25
Pentatriacontane	C_{35}	0.241	0	0.241
Hexatriacontane plus	C_{36+}	2.213	0	2.1084
Balance		100	100	100

Table 21

Results of flash calculation on a delumped system using PVTsim software at a pressure (P) of 0.1 MPa and a temperature (T) of 303.37 K

Component		Total	Vapor	Liquid
		Mole, %	Mole, %	Mole, %
Nitrogen	N_2	0.12	81.865	0.119
Carbon dioxide	CO_2	0.001	0.077	0.001
Hydrogen sulfide	H_2S	0	0	0
Methane	C_1	0	0	0
Ethane	C_2	0	0	0
Propane	C_3	0.002	0.02	0.002
Isobutane	iC_4	2.283	9.256	2.283
Butane	nC_4	0.005	0.014	0.005
Isopentane	iC_5	3.096	3.467	3.096
Pentane	nC_5	2.594	2.189	2.594
Hexane	C_6	4.485	1.19	4.485
Heptane	C_7	9.89	1.04	9.89
Octane	C_8	14.949	0.69	14.949
Nonane	C_9	7.51	0.125	7.51
Dean	C_{10}	6.93	0.045	6.93
Undecane	C_{11}	5.728	0.015	5.728
Dodecane	C_{12}	4.83	0.005	4.83
Tridecane	C_{13}	4.436	0.001	4.436
Tetradecane	C_{14}	3.757	0.001	3.757
Pentadecane	C_{15}	3.938	0	3.938
Hexadecane	C_{16}	3.091	0	3.091
Heptadecane	C_{17}	2.672	0	2.672
Octadecane	C_{18}	2.487	0	2.488
Nonadecane	C_{19}	2.127	0	2.127
Icosane	C_{20}	1.83	0	1.83
Heneicosane	C_{21}	1.611	0	1.611
Docosane	C_{22}	1.386	0	1.386
Triclosan	C_{23}	1.229	0	1.229
Tetracosane	C_{24}	1.022	0	1.022
Pentacosane	C_{25}	0.922	0	0.922
Hexacosane	C_{26}	0.795	0	0.795
Heptacosane	C_{27}	0.712	0	0.712
Octacosane	C_{28}	0.619	0	0.619
Nonacosane	C_{29}	0.604	0	0.604
Triacontane	C_{30}	0.476	0	0.476
Hentriacontane	C_{31}	0.444	0	0.444
Dotriacontane	C_{32}	0.367	0	0.367
Tritriacontane	C_{33}	0.342	0	0.342
Tetratriacontane	C_{34}	0.25	0	0.25
Pentatriacontane	C_{35}	0.241	0	0.241
Hexatriacontane plus	C_{36+}	2.213	0	2.213
Balance		100	100	100

5. 5. Comparison of the experimental, numerical and simulation results

Fig. 4–6 illustrate a comparison between Laboratory Analysis, Analytical Delumping and PVTsim Delumping data. By comparing the produced grouping mixture to field data, the obtained grouping mixture was verified. The outcomes of analytical and numerical ungrouping techniques were validated by comparing crucial properties of the components with laboratory PVT data and relevant literature data. The analytical delumping approach gives more accurate results for flash calculations compared to PVTsim due to the usage of the Newton-Raphson equation, which is not included in the series of equations of the program.

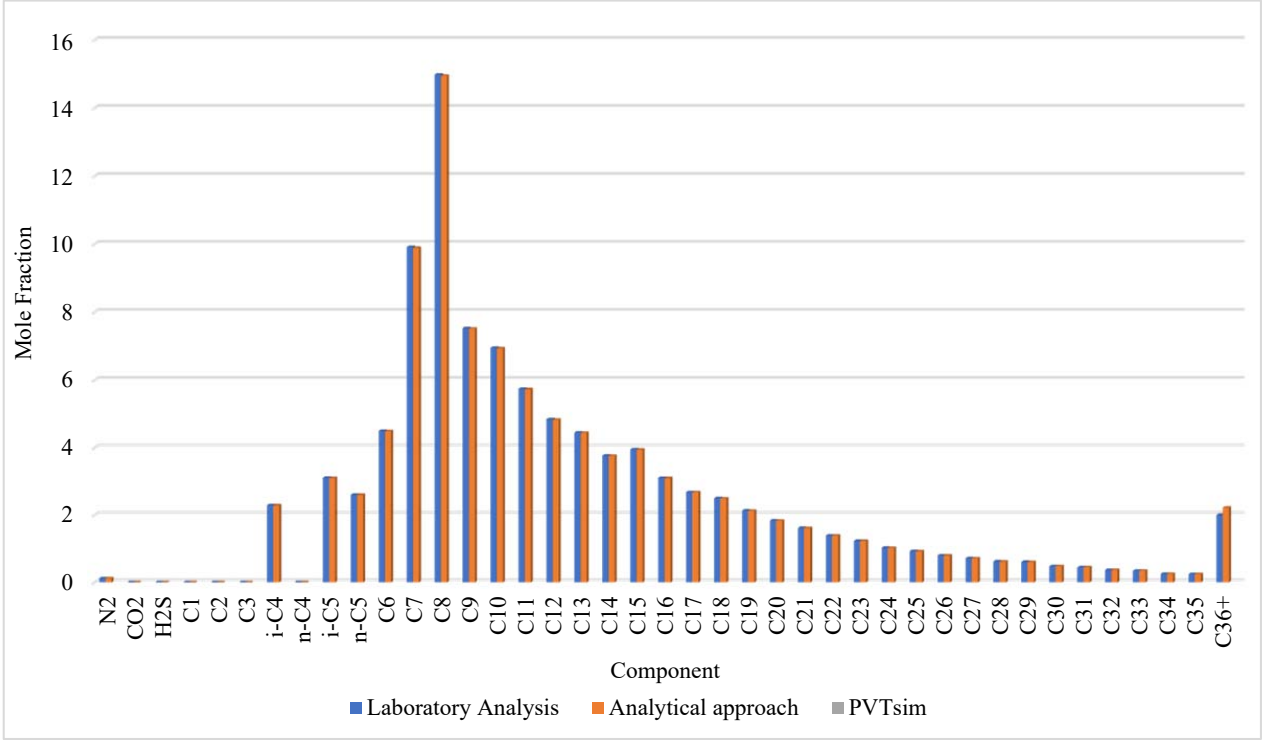

Fig. 4. Mole Fraction of the Laboratory analyzed fluid and Delumped Fluid chart

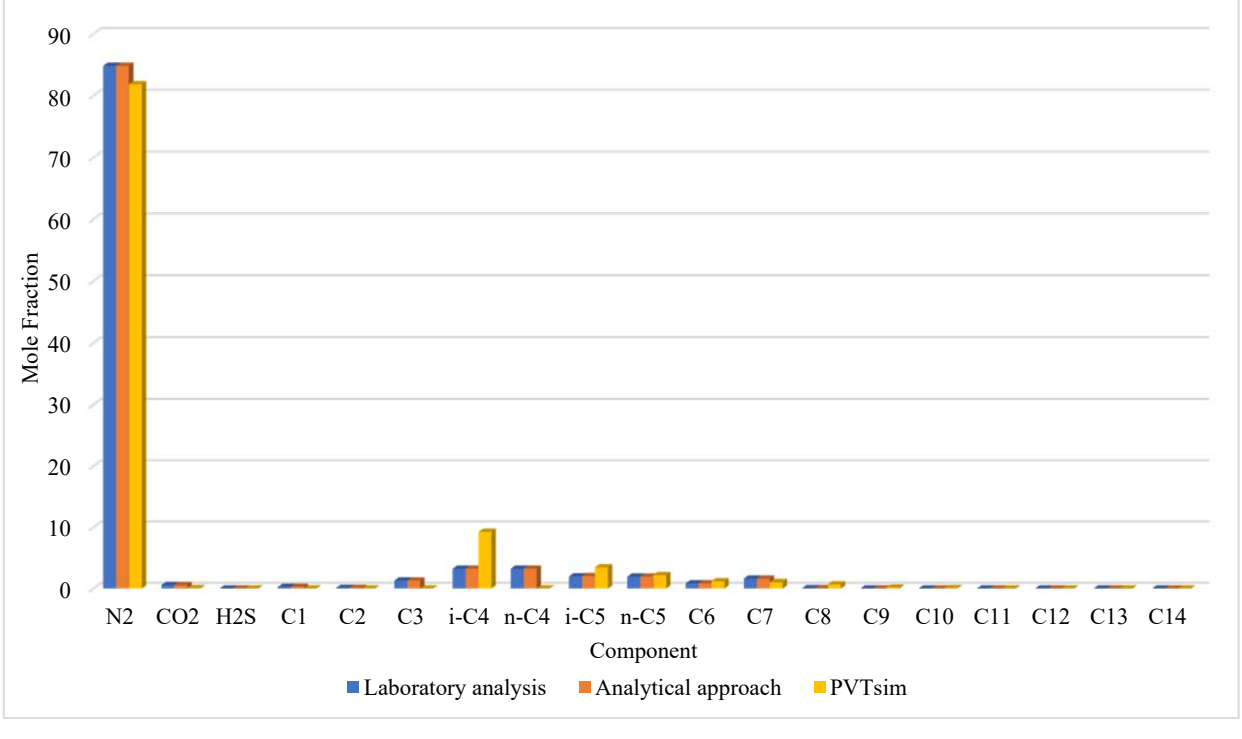

Fig. 5. Mole fraction of the Laboratory analyzed fluid and Delumped Fluid (Vapor phase)

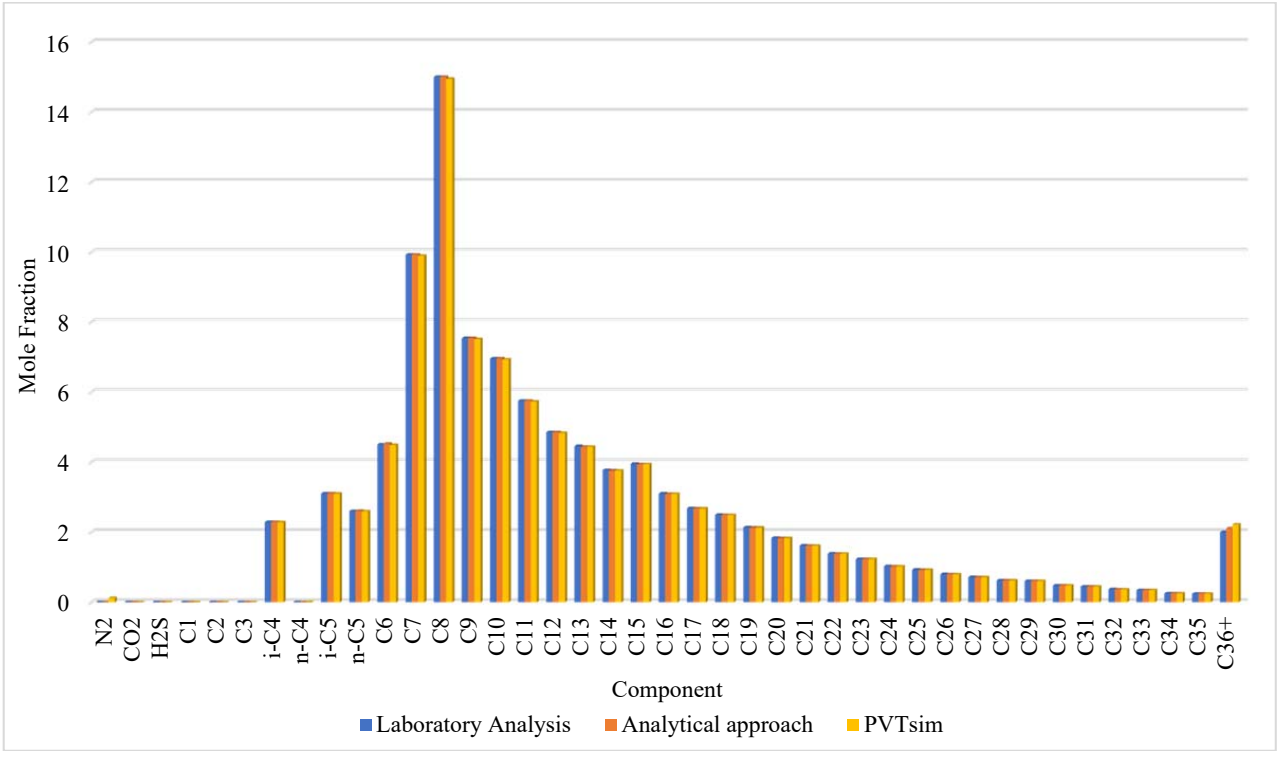

Fig. 6. Liquid Phase Mole fraction of the Laboratory analyzed fluid and Delumped Fluid (Liquid Phase)

Fig. 4–6 show a match between laboratory analysis, analytical delumping and PVTsim delumping.

6. Discussion of the results of fluid characterization

Based on the data highlighted in Fig. 4–6, it can be seen that calculations made manually by the analytical delumping approach are very close to the values obtained during laboratory analysis. There are some deviations in the PVTsim program results. However, based on Tables 20, 21 and the graphs, the same trend of mole fraction range, reducing the gas fraction of the components and increasing the proportion of its liquid phase with the growth of carbon number is clearly visible. Starting from C_{13} and ending with C_{36+}, the components are only in the liquid phase.

Our research can be linked to the research presented in [8], which improved upon the LSK approach and introduced an analytical reduction-based delumping technique. This approach proved effective in handling scenarios with non-zero BICs. Our research aligns with the aim of addressing non-zero BICs and the need for analytical delumping. It reinforces the significance of the analytical delumping approach compared to regression-based methods [8].

Our findings also can be compared to studies such as [6] that employed the LBW delumping approach for reservoir simulation. This study showed promising results when BIPs were set to zero. However, it highlighted the challenges of dealing with non-zero BIPs, which is an area our research sought to address. The agreement we found in our work, particularly for heavier components, demonstrates the feasibility of analytical delumping even when non-zero BICs are present.

However, it's crucial to acknowledge certain limitations. Primarily, this study revolves around a specific oil sample, potentially limiting its capacity to encapsulate the entire spectrum of behaviors observed in distinct oil reservoirs. The research primarily centers on Caspian basin oil, making it essential to recognize that the findings may not seamlessly translate to oils from disparate regions characterized by distinct compositions and properties. Additionally, the utilization of numerical modeling tools such as PVTsim inherently relies on a set of assumptions and equations of state. Any disparities between these model assumptions and real-world conditions have the potential to impact the accuracy of the results. These considerations underscore the need for cautious interpretation and recognition of potential constraints in our study's scope and applicability.

Furthermore, the delumping approach is appropriate for nonzero BIPs between individual components and zero BIPs between groups. If all BIPs between components within groups are zero, an analytical approach is also available for non-zero BIPs between groups. As a result, the ungrouping procedure enables the restoration of phase equilibrium of a complete mixture utilizing just the results of phase equilibrium calculations for lumped mixtures composed of discrete and pseudo-components. The approach, which relies on the reduction parameters, that takes into account non-zero BIPs can be used as a foundation for ungrouping procedures.

Following that, based on the delumping of composite modeling data and its successful validation with laboratory data and relevant literature sources, new software can be produced and implemented as an embedded algorithm, not a post-processor. The implementation of delumping of composite modeling results not as a postprocessor but as an internal program will allow you to simulate the behavior of the fluid and use the output data for planning and construction of structures quickly and accurately. From the technological point of view, the developed analytical tool can be used to predict reservoir fluid composition at any conditions as well as input data for planning and construction of the surface facilities in Kazakhstan and around

the world. By reducing the number of components into groups of pseudo-components involved in calculations, it is possible to reduce the time of calculations. This is especially important in the case of a large amount of data when processing and analyzing all components. This algorithm allows you to obtain an accurate analysis of the component composition of oil while saving time and money on laboratory research. The study of the composition of oil makes it possible to better understand its structure and properties, which in turn can lead to the development of new technologies and products based on oil.

7. Conclusions

1. In pursuit of a comprehensive understanding of Caspian basin oil, the research team conducted a series of vital laboratory experiments. These experiments, including flash liberation and constant mass expansion tests, were implemented to characterize the behavior and composition of this oil. As a result of these experiments, we obtained essential data crucial for fluid characterization, extending up to C_{36+} and encompassing liberated gas and stabilized oil. Moreover, the research successfully determined basic oil parameters. These findings were instrumental in enabling precise numerical calculations.

2. The study successfully employed the Gamma Distribution Model to describe molar distributions of components. The best-fit parameter γ was found to be 0.5, which was then used for lumping pseudo-components. This approach allowed for the effective grouping of components into pseudo-components based on their molar characteristics. The obtained model was customized to match the specific characteristics of the C_{7+} tail, enhancing the accuracy of lumping.

3. The delumping of the composite modeling results was conducted using an analytical approach with non-zero BIPs. Critical parameters, such as acentric factors, critical pressure, critical temperature, parameters 'a' and 'b' for each component were estimated at this stage. The accuracy of the delumping approach was tested by simulation.

4. Simulations of delumping and lumping procedures were successfully conducted using PVTsim software for reservoir fluid characterization. The results have demonstrated close agreement between the calculated and simulated data, which are demonstrated in Tables 20, 21. As evident from the quantitative comparison, there is generally a good agreement between the two methods for components such as N_2, CO_2, and H_2S, with deviations in the range of a few percentage points. However, for components such as methane to butane, there are significant discrepancies, with deviations exceeding 1 %. The results appear to be within an acceptable range.

5. Calculations made manually by the analytical delumping approach are very close to the values obtained during laboratory analysis. There are some deviations in the PVTsim program results. However, the same trend of mole fraction range, reducing the gas fraction of the components and the proportion of its liquid phase with the growth of carbon number is clearly visible. This comparison confirmed the effectiveness of the modeling approach and validated the accuracy of the results.

Conflict of interest

The authors declare that they have no conflict of interest in relation to this research, whether financial, personal, authorship or otherwise, that could affect the research and its results presented in this paper.

Financing

The study was conducted within the Grant Funding competition for young scientists on scientific and (or) scientific and technical projects for 2021-2023 under the Ministry of Science and Higher Education of the Republic of Kazakhstan. Project name: "Development of PVT model for prediction of wax precipitation", No. AP09058452.

Data availability

Data will be made available on reasonable request.

References

1. Assareh, M., Ghotbi, C., Pishvaie, M. R., Mittermeir, G. M. (2013). An analytical delumping methodology for PC-SAFT with application to reservoir fluids. Fluid Phase Equilibria, 339, 40–51. doi: https://doi.org/10.1016/j.fluid.2012.11.025
2. Nichita, D. V., Broseta, D., Leibovici, C. F. (2007). Reservoir fluid applications of a pseudo-component delumping new analytical procedure. Journal of Petroleum Science and Engineering, 59 (1-2), 59–72. doi: https://doi.org/10.1016/j.petrol.2007.03.003
3. Schlijper, A. G., Drohm, J. K. (1988). Inverse Lumping: Estimating Compositional Data From Lumped Information. SPE Reservoir Engineering, 3 (03), 1083–1089. doi: https://doi.org/10.2118/14267-pa
4. Danesh, A., Xu, D., Todd, A. C. (1992). A Grouping Method To Optimize Oil Description for Compositional Simulation of Gas-Injection Processes. SPE Reservoir Engineering, 7 (03), 343–348. doi: https://doi.org/10.2118/20745-pa
5. Leibovici, C., Stenby, E. H., Knudsen, K. (1996). A consistent procedure for pseudo-component delumping. Fluid Phase Equilibria, 117 (1-2), 225–232. doi: https://doi.org/10.1016/0378-3812(95)02957-5
6. Leibovici, C. F., Barker, J. W., Wach , D. (2000). Method for Delumping the Results of Compositional Reservoir Simulation. SPE Journal, 5 (02), 227–235. doi: https://doi.org/10.2118/64001-pa
7. Nichita, D. V., Leibovici, C. F. (2006). An analytical consistent pseudo-component delumping procedure for equations of state with non-zero binary interaction parameters. Fluid Phase Equilibria, 245 (1), 71–82. doi: https://doi.org/10.1016/j.fluid.2006.03.016
8. De Castro, D. T., Nichita, D. V., Broseta, D., Herriou, M., Barker, J. W. (2011). Improved Delumping of Compositional Simulation Results. Petroleum Science and Technology, 29 (1), 1–12. doi: https://doi.org/10.1080/10916460903330098
9. Stenby, E. H., Christensen, J. R., Knudsen, K., Leibovici, C. (1996). Application of a Delumping Procedure to Compositional Reservoir Simulations. All Days. doi: https://doi.org/10.2118/36744-ms
10. Barker, J. W., Leibovici, C. F. (1999). Delumping Compositional Reservoir Simulation Results: Theory and Applications. All Days. doi: https://doi.org/10.2118/51896-ms